CHAPTER FIVE

Optical Imaging of Treatment-related Tumor Cell Death Using a Heat Shock Protein-90 Alkylator

Based on

Park D*, Xie BW*, Van Beek ER, Blankevoort V, Que I, Löwik CW, Hogg PJ. ***Mol Pharm.*** 2013 Aug 22. [Epub ahead of print].

Abstract

The ability to assess in near-real time the tumor cell-killing efficacy of chemotherapy regimens would improve patient treatment and survival. An ineffective regimen could be abandoned early in favor of a more effective treatment. We sought to non-invasively image treatment-related tumor cell death in mice using an optically labelled synthetic heat shock protein-90 (Hsp90) alkylator, 4-(N-(S-glutathionylacetyl)amino)phenylarsonous acid (GSAO). The Hsp90 chaperone is an important element in oncogene addiction and tumor cell survival and its expression is enhanced by chemotherapy. These factors were predicted to favor the detection of tumor cell death using GSAO. Fluorescent conjugates of GSAO specifically labelled apoptotic and necrotic cancer cells in culture and a biotin conjugate of GSAO labelled cells of the same morphology in subcutaneous human pancreatic tumors in mice. A near-infrared conjugate of GSAO was further used to non-invasively image cyclophosphamide-induced tumor cell death in orthotopic murine mammary tumors in mice. The GSAO conjugate did not accumulate in healthy organs or tissues in the mouse and unbound compound was excreted rapidly via the kidneys. There was a significant increase in the GSAO fluorescence signal in the treated tumors measured either *in vivo* or *ex vivo* and the fluorescence signal co-localized with apoptotic cells in sectioned tumors. The favourable biodistribution of optically labelled GSAO, the nature of its tumor cell target and its capacity to non-invasively detect tumor cell death should facilitate the application of this compound in studies of the efficacy of existing and new chemotherapeutics.

Keywords

Tumor cell death, chemotherapy, apoptosis, necrosis, GSAO, optical imaging

Abbreviations

GSAA, 4-(*N*-(*S*-glutathionylacetyl)amino)phenylarsonic acid; GSAO, 4-(N-(S-glutathionylacetyl)amino)phenylarsonous acid; GSCA, 4-(N-((S-glutathionyl) acetyl)amino)benzoic acid; AF750, Alex Flour 750; Hsp90, heat shock protein 90; PI, propidium iodide; ROI, region of interest; TUNEL, TdT-mediated dUTP nick-end labelling

Introduction

Cancer results from an imbalance between rates of cellular proliferation and survival in a given tissue. Successful treatment controls cancer cell growth by inhibiting cellular proliferation and/or promoting cell death. Cancer patients with metastatic disease are often treated with cytotoxic chemotherapy to control tumor burden and/or to prolong life. To determine if chemotherapy is working, tumor size is usually assessed by computed tomography after six to nine weeks of treatment. This measure is used in decisions about further treatment. Being able to rapidly assess tumor cell proliferation and death in response to treatment would improve the management of this disease [1].

Technologies that monitor therapy response have and are being developed. The measure in the widest clinical use is ^{18}F-fluorodeoxyglucose-positron emission tomography (FDG-PET) [1-3]. FDG uptake in vivo, though, is a composite measure of several biological processes. Decreased FDG uptake by tumors can reflect decreased glucose utilization by viable tumor cells and/or tumor cell death [4,5]. Moreover, FDG is also taken up by inflammatory cells [4]. A robust, minimally invasive, and universally applicable measure of early tumor response to treatment would significantly enhance patient care and the pace of new pharmaceutical development [1,6]. By reporting on the efficacy of new cytotoxic drugs and possibly the toxicity of these drugs in other tissues, 'go/no go' decisions will be easier to make.

There has been a particular focus on the development of imaging agents that measure tumor cell death in response to treatment. Chemotherapy and radiotherapy can result in many different types of tumor cell death, including apoptosis, necrosis, autophagy, mitotic catastrophe and cell senescence [7-9]. Probes that detect exteriorized phosphatidylserine on the surface of apoptotic cells [10-18], activated caspase-3/7 in apoptotic cells [19] and a ribonucleoprotein exposed during apoptotic and necrotic cell death [20,21] have been tested as indicators of treatment-related tumor cell death.

In this study we have tested an optically labelled small molecule alkylator of heat shock protein-90 (Hsp90) as an indicator of response to tumor treatment in mice. The in principle advantages of this compound is that it selectively recognizes both apoptotic and necrotic cell death and its tumor target, Hsp90, is an abundant cytoplasmic chaperone that plays a fundamental role in tumorigenesis. The Hsp90 chaperone machine protects a number of mutated and overexpressed oncoproteins from misfolding and degradation [22,23]. As such, it is considered an important factor in oncogene addiction and tumor cell survival. In addition, the cellular expression of Hsp90 increases in response to stresses such as hypoxia and chemotherapeutics in an attempt to restore cellular homeostasis [22,23].

Hsp90 contains a Cys597, Cys598 dithiol in the C-terminal domain [24] and the sulphur atoms are involved in redox reactions in the cytoplasm [25]. The Hsp90

alkylator is a tripeptide trivalent arsenical called GSAO (4-(N-(S-glutathionylacetyl) amino)phenylarsonous acid). The As(III) atom of GSAO cross-links the Cys597, Cys598 dithiol of Hsp90, forming a stable cyclic dithioarsinite that is effectively irreversible in biological milieu. When tagged with optical or radio reporter molecules, GSAO specifically labels dying/dead cells. The compound accumulates in the cytosol of dying cells coincident with loss of plasma membrane integrity and is retained in the cytoplasm by reacting predominantly with Hsp90 [26]. It has a favorable biodistribution in the living animal and is cleared quickly from the circulation via the kidneys [27]. In this study, a near-infrared conjugate of GSAO has been used to non-invasively image cyclophosphamide-induced cell death in breast carcinoma tumors in mice.

Results

Fluorescent conjugates of GSAO have been shown to label apoptotic and necrotic cells [26,27]. We sought to confirm the specificity of this labelling using a T cell hybridoma cell line and to define the cellular distribution of the labelling. The cell death targeting specificity of GSAO in labelling dying/dead cells in culture was examined, followed by validating its targeting specificity in labelling apoptotic and necrotic tissues in solid tumors in mice.

GSAO-OG specifically labels apoptotic and necrotic cells in culture

The microbial alkaloid, staurosporine, is a broad spectrum protein kinase inhibitor that activates the intrinsic/mitochondrial-mediated pathway of apoptotic cell death [28,29], while freeze/thaw ruptures the plasma membrane resulting in necrotic cell death [30].

Apoptotic and necrotic Jurkat T cells were labelled with GSAO-OG and the late stage apoptosis/necrosis marker, propidium iodide (PI). GSAO-OG labelled PI-positive cells resulting from both types of cell death (Fig. 1, upper panel). There were subpopulations of cells that labelled with GSAO-OG and not PI and vice versa, but these were <10% of the total cell population. The selectivity of GSAO-OG for apoptotic and necrotic cells is mediated by the trivalent arsenic moiety, as has been described previously [26,27]. This was confirmed using control GSCA-OG that contains a chemically inert carboxylic acid group in place of the reactive trivalent arsenic moiety. GSCA-OG did not label apoptotic or necrotic PI-positive cells (Fig. 1, lower panel).

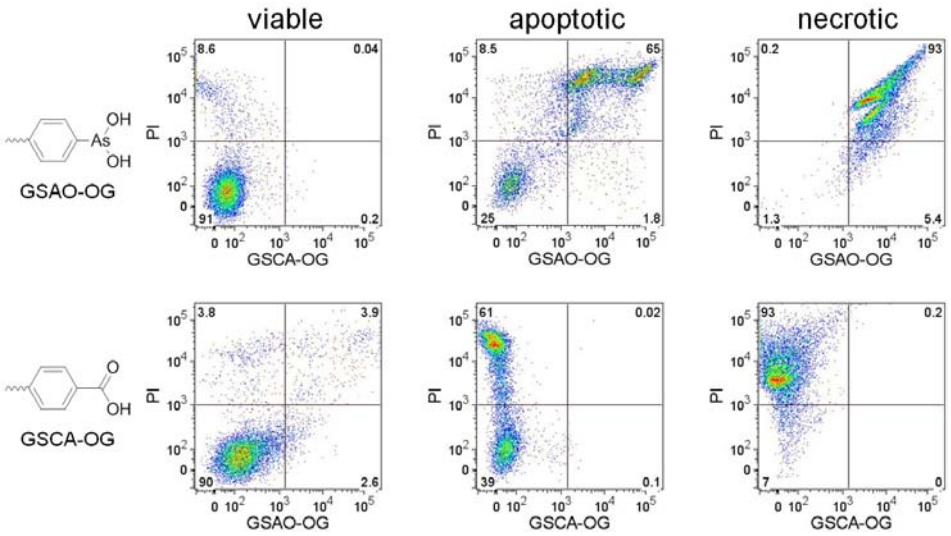

Figure 1. GSAO-OG specifically labels apoptotic and necrotic cells in culture. Apoptotic or necrotic death of Jurkat A3 T cells was triggered with staurosporine or freeze/thaw, respectively. The cells were subsequently incubated with PI (all panels) and either GSAO-OG (upper panels) or control GSCA-OG (lower panels) and labelling analysed by flow cytometry. The numbers depicted in the scatter plots represent the percentage of cells in the quadrants.

GSAO-OG labels the cytoplasm of apoptotic and necrotic cells in culture

To determine the subcellular localization of GSAO-OG, apoptotic or necrotic Jurkat T cells were incubated with GSAO-OG, the phosphatidylserine ligand, annexin V-APC, and the nucleic acid stain, DAPI. The cells were imaged by confocal microscopy. GSAO-OG distributed in the cytoplasm of annexin V-positive apoptotic cells and the necrotic cell fragments resulting from freeze/thaw (Fig. 2). Only a few cell necrotic cell fragments labelled with annexin V, although most labelled with DAPI indicating the presence of nuclei.

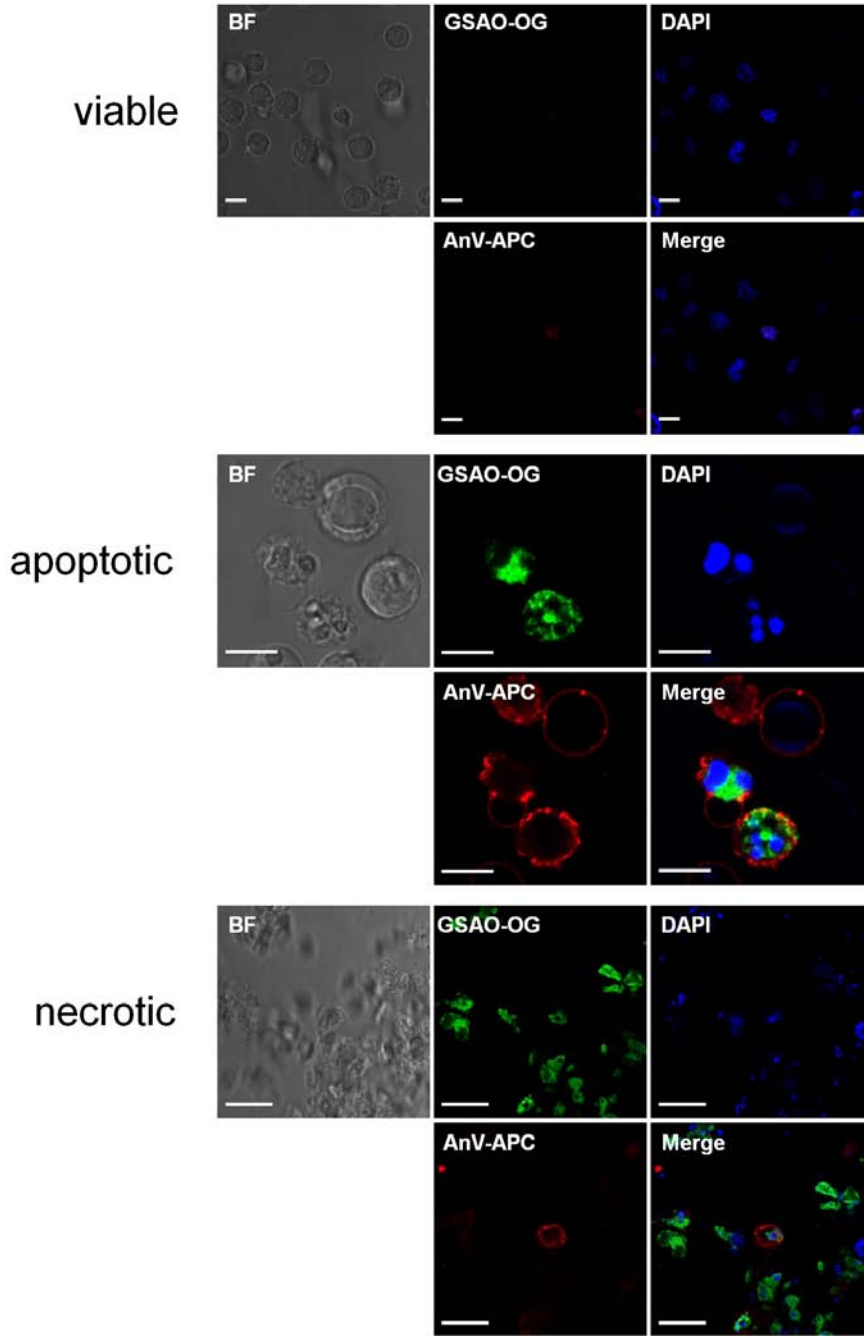

Figure 2. GSAO-OG labels the cytoplasm of apoptotic and necrotic cells in culture. Apoptotic or necrotic death of Jurkat A3 T cells was triggered with staurosporine or freeze/thaw, respectively. The cells were subsequently incubated with GSAO-OG (green), DAPI (blue) and annexin V-APC (red) and imaged by confocal microscopy. The bottom right-hand images are a merge of all three colors. The bar represents 20 µm.

GSAO-biotin labels tumor cells of apoptotic and necrotic morphology *in vivo*

We next sought to identify the morphology of GSAO-labelled cells in tumors. Biotin-tagged GSAO was administered to immunodeficient mice bearing subcutaneous human pancreatic carcinoma tumors. The tumors were excised 6 h later and sections stained for the biotin moiety of the label using streptavidin-peroxidase, and counterstained with haematoxylin to identify viable tumor cells. This method allowed for a better characterization of the tumor morphology and labelled regions that could be revealed using fluorescent conjugates of GSAO. There was an accumulation of GSAO-biotin in regions of the tumor where apoptotic and necrotic cells were prevalent (Fig. 3). GSAO-biotin stained cells that showed signs of apoptosis, including a condensed nucleus and shrunken cytoplasm, and cell fragments that resemble the necrotic fragments labelled by GSAO-OG in culture (see Fig. 2). There was no staining of viable tumor cells by GSAO-biotin. There was no detectable control GSAA-biotin in tumor sections from mice administered with this compound (not shown).

The capacity of an optically labelled GSAO to image treatment-related cell death in murine tumors was investigated. The treatment model was first established using immunodeficient mice bearing orthotopic mammary carcinoma tumors. This tumor model was selected for two reasons. First, orthotopic inoculation of 4T1 breast cancer cells can result in the spontaneous generation of lung, liver, bone and brain metastases, mimicking progression of the disease in humans [31-33]. Second, tumor growth in the mammary fat pad provides a more relevant microenvironment than subcutaneous models. This is particularly important with regard to the tumor vasculature, as tagged GSAO is administered intravenously, and the architecture and organization of the vascular network will influence probe dissemination and thus uptake. Variation in tumor vessel density, diameter and/or permeability has been observed in mouse models of renal cell carcinoma, melanoma, glioblastoma, mammary carcinoma, hepatoma and fibrosarcoma depending on the site of implantation [32-35]. The chemotherapeutic employed was cyclophosphamide, a DNA alkylating agent that is used to treat breast cancer [35,36]. This tumor treatment model, therefore, is a clinically relevant system in which to test GSAO imaging of tumor cell death.

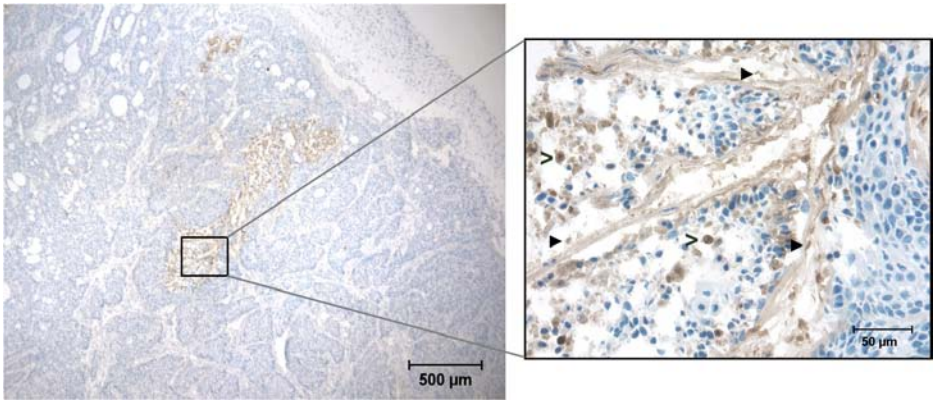

Figure 3. GSAO-biotin labels tumor cells of apoptotic and necrotic morphology in vivo. Mice bearing subcutaneous BxPC-3 tumors in the proximal dorsum were administered GSAO-biotin or control GSAA-biotin by subcutaneous injection in the hind flank. The tumors were excised after 6 h, sectioned and stained for GSAO-biotin using streptavidin-peroxidase (brown color) and co-stained with haematoxylin to reveal viable tumor cells (blue color). Shown is a low and high power micrograph of a sectioned tumor demonstrating incorporation of GSAO-biotin into cells of apoptotic (open arrowheads) and necrotic morphology (closed arrowheads). There was no detectable labelling of tumors with control GSAA-biotin.

Establishment of the tumor treatment model

Nude mice bearing orthotopic 4T1-luc2 mammary carcinoma tumors were untreated or treated with a single intravenous injection of 250 mg/kg cyclophosphamide, and 24 h later the tumors were imaged by bioluminescence and then excised and weighed. There was a statistically significant reduction in the size of the treated tumors measured either *in vivo* by bioluminescence (Fig. 4A, $p < 0.01$) or *ex vivo* by weight (Fig. 4B, $p < 0.01$). There were no signs or symptoms of toxicity of the cyclophosphamide in this experimental design. This result indicated that the cyclophosphamide was impairing the proliferation and/or inducing death of the tumor cells over the 24 hour period. We then sought to non-invasively image the tumor cell death using the near infrared fluorescent conjugate of GSAO, GSAO-AF750.

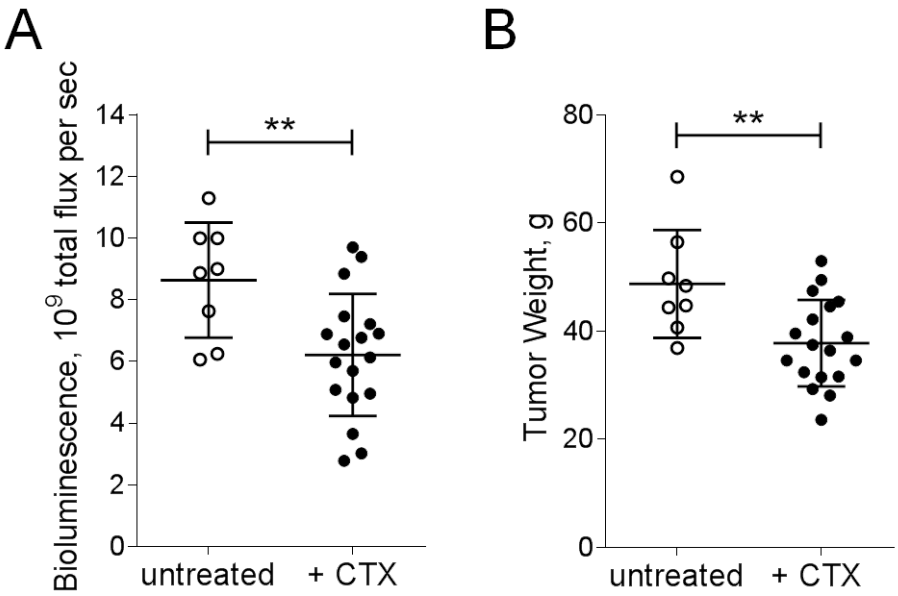

Figure 4. Establishment of the tumor treatment model. Nude mice bearing orthotopic 4T1-luc2 mammary carcinoma tumors were untreated or treated with 250 mg/kg cyclophosphamide (CTX). After 24 h, the mice were injected with D-luciferin and imaged for bioluminescent signals and then sacrificed and the tumors excised and weighed. Results are the mean ± SD of a total of 18 mice from two separate experiments. **, $p < 0.01$.

Non-invasive imaging of treatment-related tumor cell death using GSAO-AF750

Nude mice bearing orthotopic 4T1-luc2 mammary carcinoma tumors were untreated or treated with 250 mg/kg cyclophosphamide for 24 h as described above. The mice then received a tail vein injection of either 1 mg/kg GSAO-AF750 or control GSCA-AF750 and 60 min later whole body fluorescence images were acquired (Fig. 5A). The tumors were excised three hours later and fluorescence images acquired *ex vivo*. There was a statistically significant increase in the GSAO-AF750 signal in the treated tumors measured either *in vivo* (Fig. 5B, $p < 0.01$) or *ex vivo* three hours later (Fig. 5C, $p < 0.05$). The signal from control GSCA-AF750 in treated tumors was substantially lower in both settings (Fig. 5B and C, $p < 0.001$).

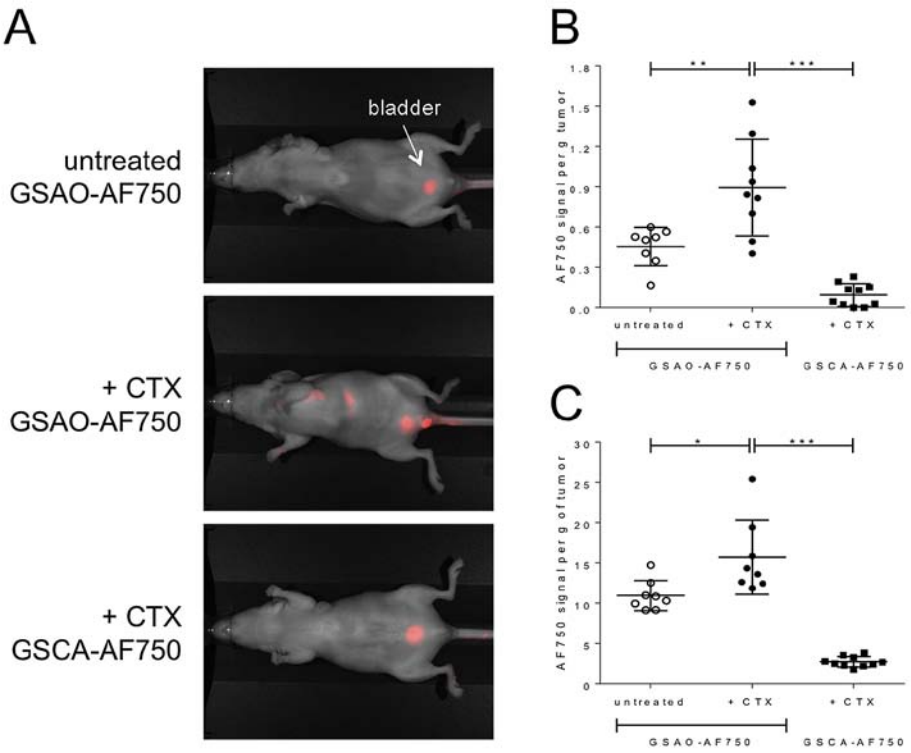

Figure 5. Non-invasive imaging of treatment-related tumor cell death using GSAO-AF750. Nude mice bearing orthotopic 4T1-luc2 mammary carcinoma tumors were untreated or treated with 250 mg/kg cyclophosphamide (CTX). After 24 h, the mice were injected with either GSAO-AF750 or control GSCA-AF750, and whole body fluorescence images of the mice were acquired 60 min later. Three hours later the tumors were excised and fluorescence values acquired *ex vivo*. A. Representative fluorescence images of whole mice. A fluorescence signal is observed in the treated tumor and in the kidneys/bladders of all mice, where GSAO-AF750 is excreted. B. Quantitation of the *in vivo* tumor fluorescent intensity, expressed as AF750 signal intensity per gram of tumor. C. Quantitation of the *ex vivo* tumor fluorescent intensity, expressed as AF750 signal per gram of tumor. Results are the mean ± SD of a total of 10 mice from two separate experiments. ***, $p < 0.001$; **, $p < 0.01$; *, $p < 0.05$.

GSAO-AF750 labels apoptotic cells in the mammary carcinoma tumors

The excised tumors from the experiment described above were sectioned and apoptotic cells visualised by TUNEL staining or with an antibody that recognises activated caspase-3. TUNEL-positive regions of the untreated and treated tumors were strongly positive for GSAO-AF750, which was more pronounced in the treated tumors (Fig. 6A). Individual apoptotic tumor cells were co-labelled with activated caspase-3 antibody staining and GSAO-AF750 (Fig. 6B). There was no labelling of tumors with control GSCA-AF750 (Fig. 6A and B).

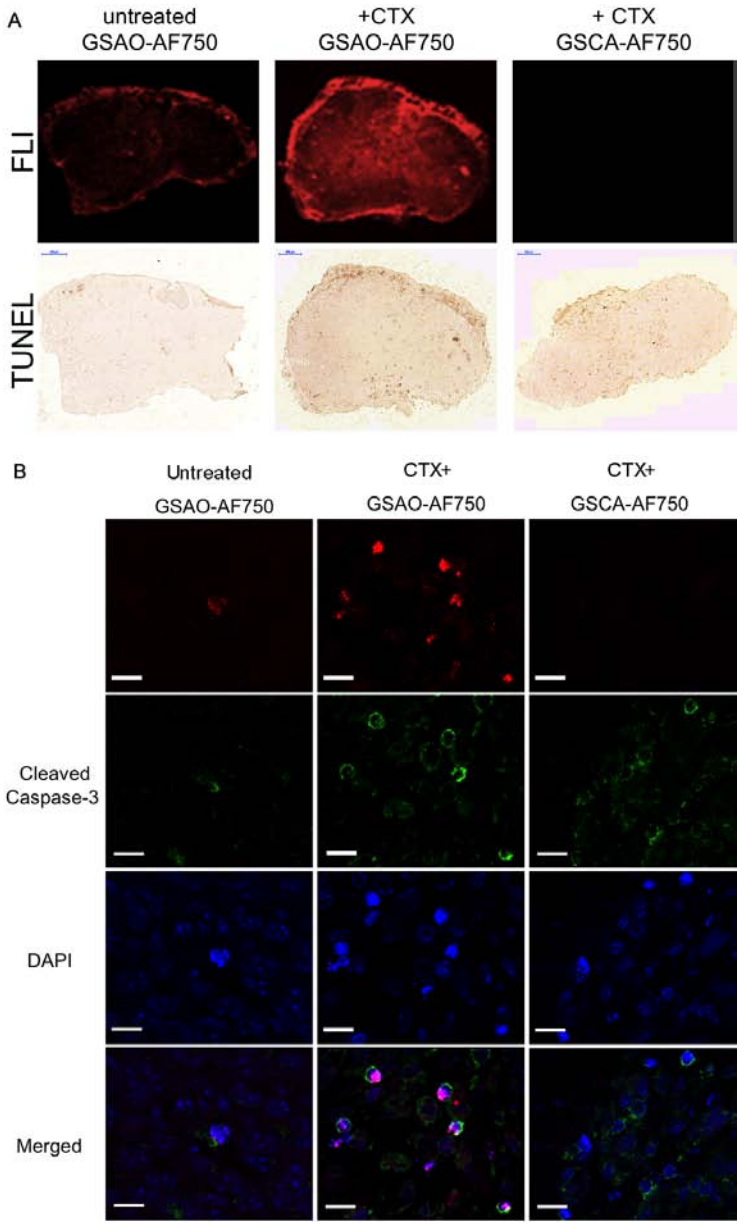

Figure 6. GSAO-AF750 labels apoptotic cells in the mammary carcinoma tumors. Nude mice bearing orthotopic 4T1-luc2 mammary carcinoma tumors were untreated or treated with 250 mg/kg cyclophosphamide (CTX). After 24 h, the mice were injected with either GSAO-AF750 or control GSCA-AF750, and three hours later the tumors were excised. Tumors were sectioned and apoptotic cells visualized by TUNEL staining or with an anti-activated caspase-3 antibody. Cell nuclei were stained with DAPI. A. Whole tumor sections showing the co-localization between GSAO-AF750 fluorescence and TUNEL-positive regions. B. Consecutive tumor sections showing co-labelling of cells with GSAO-AF750 and activated caspase-3 antibody. There was no labelling of tumors with control GSCA-AF750. The bar represents 40 µm.

Discussion

A robust and universally applicable measure of early tumor response to treatment would be a valuable tool for patient care and new pharmaceutical discovery, however there are challenges in developing this technology. The main issues are a cell death marker with the appropriate specificity, sensitivity and biodistribution, the nature and timing of the treatment-induced cell death, and distinguishing between the basal and treatment-related tumor cell death. These challenges will be considered in turn.

Phosphatidylserine is exposed on the exterior of the plasma membrane during apoptosis and four different phosphatidylserine ligands have been evaluated for the measurement of treatment-related tumor cell death. The first of these is the protein annexin V, which binds to phosphatidylserine in the presence of calcium ions [37]. An optically and radiolabelled annexin V has been evaluated in mice [10-13]. Some factors that have limited the adoption of annexin V include its large size (>35 kDa), which can result in slow delivery and clearance from the cells of interest, and high renal uptake. The C2A domain of synaptotagmin I binds phosphatidylserine and a radiolabelled molecule has been evaluated using SPECT [14] and MRI [15] imaging. Although the smaller size of this agent (~15 kDa) improves the penetration of tumor tissue, it binds phosphatidylserine with at least two orders of magnitude lower affinity than annexin V and has high hepatic and renal uptake that precludes imaging in the abdominal region. The third agent is zinc(II)-dipicolylamine that binds phosphatidylserine comparably to annexin V and has lower renal uptake, although it also binds bacteria [16,17]. A radiolabelled 14-residue phosphatidylserine-binding peptide has also been developed that labels melanoma tumors in mice and uptake is increased following paclitaxel treatment [18]. A general issue with the phosphatidylserine ligands is cross-reactivity with exteriorised phosphatidylserine in activated platelets, macrophages, endothelial cells and aging erythrocytes. Non-tumor cells under stress, such as hypoxia, will also transiently expose phosphatidylserine, which could lead to overestimation of tumor cell death.

Caspases are cysteine proteases that cleave a range of key structural proteins during the execution phase of apoptosis [38]. Caspase-3 is a central effector caspase in the demolition and clearance of apoptotic cells [39]. A radiolabelled small molecule inhibitor of activated caspase-3/7, an isatin-5 sulfonamide called ICMT-11, has been used to image treatment-related lymphoma cell death in mice by PET [19]. High hepatic uptake of the agent precludes imaging of abdominal region, though, and there is possible cross-reactivity with cathepsins. La antigen is involved in different aspects of RNA metabolism and during apoptosis translocates from the nucleus to cytoplasm [40], where it is fixed in dying cells by transglutaminase 2 [20]. Cytoplasmic La becomes accessible to antibodies when the integrity of the plasma membrane is compromised during the late phase of apoptosis [20,21]. A radiolabelled anti-La antibody has been developed (APOMAB) that shows promise for SPECT

imaging of tumor cell death in response to DNA damaging agents [20,21]. In this study, our immunohistology staining of treated tumor sections showed that even there was certain level of co-labelling between GSAO-AF750 and activated caspase-3, there were more cells with caspase-3 staining, indicating that GSAO-AF750 more specifically located in the late apoptotic and/or necrotic cells. This result confirms our previous study that GSAO that accumulates in the cytosol of dying and dead cells, coincident with loss of plasma membrane integrity [26].

Optically tagged GSAO appears to overcome some of the disadvantages of these agents. It is highly selective for both apoptotic and necrotic cells and is rapidly cleared from the mouse body, being only found in the kidneys and bladder 3 h after intravenous administration to healthy animals [27]. In addition, the abundance of Hsp90 in the cytoplasm leads to high accumulation of GSAO in dying/dead cells, which results in good imaging sensitivity and resolution. The ligands that target phosphatidylserine exposed on the exterior of the plasma membrane during apoptosis, for example, are restricted to the cell surface compartment.

For wide applicability, a tumor cell death marker should ideally report on the different types of cell death mediated by different treatments. The phosphatidylserine and activated caspase- 3 ligands were designed to image apoptotic cell death, although there is likely some cross-recognition of necrotic cell death [37]. The anti-La antibody and GSAO recognize both apoptotic and necrotic cell death, however the anti-La antibody may only image tumor cell death mediated by DNA damaging agents [20,21]. To our knowledge, there are currently no agents that image treatment-mediated tumor cell autophagy, mitotic catastrophe or cell senescence.

Perhaps the greatest challenge for this technology, though, is reliably distinguishing between basal and treatment-related cell death. Solid tumors generally contain large numbers of dying and dead cells, which is due to the naturally high rate of tumor cell death coupled with slow rate of clearance of dying and dead cells from tumors. In this study, cyclophosphamide treatment of the mammary carcinoma tumors resulted in a ~2-fold increase in tumor cell death as reported by GSAO-AF750. There was significant basal tumor cell death as indicated by the difference between GSAO-AF750 and control GSCA-AF750 labelling and the basal tumor cell death was also shown in the TUNEL staining (Fig. 6A). This magnitude of increase is in the range of other studies using different tumor treatment models and different cell death probes [10-21].

A ~10-fold differential between basal and treatment-induced tumor cell death is perhaps required before an unambiguous assessment of treatment efficacy can be made. A solution to this problem may lie in suppressing the signal from basal tumor cell death. For instance, unlabelled (or cold) GSAO could be administered a day before treatment, which would block the Hsp90 binding sites in the basal dying/dead cells and allow for clearance of the compound from the

body. The day after treatment, tagged GSAO could be administered to detect the treatment-related cell death plus any basal cell death since treatment. The differential between basal and treatment-induced tumor cell death is predicted to be greater than that observed without the pre-blocking. This hypothesis will be tested in future studies. This scenario could also be applied to other cell death imaging agents.

Materials and Methods

Conjugates of GSAO, GSCA and GSAA

Conjugates of GSAO, GSCA and GSAA with Oregon Green 488 (λ_{ex}:496 nm, λ_{em}:542 nm), Alex Flour 750 (λ_{ex}:752 nm, λ_{em}:776 nm) or Biotin-XX, SE (Life Technologies, Victoria, Australia) were made and tested for purity as described previously [26,27,41].

Labelling or apoptotic and necrotic cells with GSAO-OG

Jurkat A3 cells (ATCC, Manassas, VA) were cultured in RPMI-1640 medium supplemented with 10% fetal bovine serum and 1 U/mL penicillin/streptomycin. The cells were seeded at a density of 5 x 10^5 cells per mL and untreated or incubated with 4 µM staurosporine (Sigma) for 24 h or freeze/thawed 3 times. Cells were washed twice with ice cold phosphate-buffered saline and incubated at room temperature with 1 µM GSAO-OG or control GSCA-OG for 15 min with shaking. Cells were washed again and incubated with PI (1 µg/mL, Invitrogen) for 10 min in the dark. Flow cytometry was performed using a FACS Canto II Flow Cytometer (Becton Dickinson, Franklin Lakes, NJ) and data analyzed using FlowJo software version 8.7.

Confocal microscopic analysis of apoptotic and necrotic cells

Jurkat A3 cells were prepared as above and then incubated in 10 mM Hepes, pH 7.4 buffer containing 0.14 M NaCl and 2.5 mM $CaCl_2$ and 5 µL per 100 µL annexin V-APC (Becton Dickinson). Cells were washed twice and then incubated with DAPI/AntiFade Reagent-Prolong Gold (Life Technologies). Cells (1 x 10^5) were transferred into FD35-100 Fluorodish Cell Culture Dishes (Coherent Scientific, South Australia, Australia) and images captured using a Leica TCS SP5 inverted laser-scanning confocal microscope running Leica LAS software.

Labelling of apoptotic/necrotic tumor cells in mice with GSAO-biotin

Human pancreatic carcinoma Bx-PC3 cells (ATCC) were cultured in RPMI-1640 medium supplemented with 10% fetal bovine serum and 1 U/mL penicillin/streptomycin. A suspension of 2.5 x 10^6 cells in 0.2 mL of phosphate-buffered saline was injected subcutaneously in the proximal midline dorsum of BALB/*c nu/nu* mice (Biological Resources Centre, University of New South Wales, Sydney). Tumors were allowed to establish and grow to a size of ~1 cm^3 after which the mice were administered 36 mg/kg GSAO-biotin or control GSAA-biotin in 0.2 mL of phosphate-buffered saline containing 20 mM glycine by subcutaneous injection in the hind flank. Mice were sacrificed 6 h later and tumors were embedded in OCT compound (Sakura, Torrance, CA) and snap frozen in liquid nitrogen. Sections (5 µm) of the tumors were fixed with acetone and stained with StreptABComplex/HRP (Dako Corporation, Carpinteria, CA) according to the manufacturer's instructions. The sections were counterstained with haematoxylin and mounted with fluoromount-G (Southern Biotechnology, Birmingham, AL).

Non-invasive imaging of treatment-related tumor cell death

Mammary carcinoma 4T1-luc2 cells expressing the codon-optimized luciferase gene *luc2* (Perkin Elmer, Hopkinton, MA) were cultured in RPMI-1640 medium supplemented with 10% fetal bovine serum and 1 U/mL penicillin/streptomycin. A suspension of 0.5 × 10^6 cells in 0.1 mL of phosphate-buffered saline was injected orthotopically beneath the mammary fat pad in six-week old female BALB/*c nu/nu* mice (Charles River Laboratories, France). Seven days post tumor cell implantation mice were randomized into three groups and two groups were treated with a single tail vein injection of 250 mg/kg cyclophosphamide. The following day the mice were administered GSAO-Alexa Fluor 750 or control GSCA-Alexa Fluor 750 (1 mg/kg in 0.1 mL of phosphate-buffered saline) in the tail vein and imaged with the Pearl® Impulse Small Animal Imaging System (LI-COR Biosciences, Lincoln, NE) 1 h later. Prior to imaging, the mice were wiped with 70% v/v ethanol to remove any of the compounds excreted in the urine and contaminating the skin. At the experiment endpoint, the mice were sacrificed by cervical dislocation and the tumors excised for *ex vivo* fluorescence imaging. Images were acquired at 800 nm at a resolution of 85 µm. The fluorescent signal was digitized and electronically displayed as a pseudocolor overlay on a gray scale white light image of the animal. The data was analyzed using Pearl® Impulse Software, Version 2.0. Total AF750 fluorescence intensity was determined by drawing a ROI over the tumor. A ROI of equivalent size was then drawn over the adjacent breast to determine the background signal and this was subtracted

from the lesion signal. Tumor volume was calculated using the relationship: width x length x height x 0.523.

For bioluminescence imaging, mice received an intraperitoneal injection of 150 mg/kg D-luciferin (SynChem, Inc., Elk Grove Village, IL) in 50 µL of phosphate-buffered saline, and 10 min later were imaged using the IVIS Spectrum (Perkin Elmer, Hopkinton, MA). At the experiment endpoint the mice were sacrificed by cervical dislocation and the tumors were then excised and weighed for statistical analysis.

Ex vivo analysis of tumor labelling

The tumors were fixed in 4% formaldehyde, embedded in paraffin and 8 µm sections were prepared and imaged using the LI-COR Odyssey Infrared Imager 9120 (LI-COR Biosciences, Lincoln, NE) at 800 nm. Afterwards, the sections were subjected to TUNEL staining (DeadEnd™ Colorimetric TUNEL System, Promega Benelux, Leiden, The Netherlands) to identify the apoptotic cells. Consecutive sections were also stained for activated caspase-3 using 5A1E rabbit monoclonal antibody (Cell Signaling, Leiden, The Netherlands) and Alexa Fluor 488® Donkey anti-rabbit IgG (Invitrogen, Breda, The Netherlands), and for nuclei using DAPI (Invitrogen, Breda, The Netherlands).

Ethical statement

All animal experiments were approved for animal health, ethic and research by the Animal Welfare Committee of Leiden University Medical Center, the Netherlands (Approval DEC number 11198). All mice were purchased from Charles River Laboratories, France and received humane care and maintenance in compliance with the "Code of Practice Use of Laboratory Animals in Cancer Research" (Inspectie W&V, July 1999).

Statistical analysis

We used two-tailed, unpaired Student's t-test.

Acknowledgments

This study is supported by the Dutch Center for Translational Molecular Medicine, project MUSIS (grant 03O-202), the National Health and Medical Research Council of Australia and the Cancer Council New South Wales.

References

1. Weber, W.A., Czernin, J., Phelps, M.E. & Herschman, H.R. Technology Insight: novel imaging of molecular targets is an emerging area crucial to the development of targeted drugs. *Nature clinical practice. Oncology* **5**, 44-54 (2008).
2. Larson, S.M. & Schwartz, L.H. 18F-FDG PET as a candidate for "qualified biomarker": functional assessment of treatment response in oncology. *J. Nucl. Med.* **47**, 901-903 (2006).
3. Shankar, L.K.*, et al.* Consensus recommendations for the use of 18F-FDG PET as an indicator of therapeutic response in patients in National Cancer Institute Trials. *J. Nucl. Med.* **47**, 1059-1066 (2006).
4. Workman, P.*, et al.* Minimally invasive pharmacokinetic and pharmacodynamic technologies in hypothesis-testing clinical trials of innovative therapies. *J. Natl. Cancer Inst.* **98**, 580-598 (2006).
5. Su, H.*, et al.* Monitoring tumor glucose utilization by positron emission tomography for the prediction of treatment response to epidermal growth factor receptor kinase inhibitors. *Clin. Cancer Res.* **12**, 5659-5667 (2006).
6. Weissleder, R. & Pittet, M.J. Imaging in the era of molecular oncology. *Nature* **452**, 580-589 (2008).
7. Johnstone, R.W., Ruefli, A.A. & Lowe, S.W. Apoptosis: a link between cancer genetics and chemotherapy. *Cell* **108**, 153-164 (2002).
8. Brown, J.M. & Attardi, L.D. The role of apoptosis in cancer development and treatment response. *Nat Rev Cancer* **5**, 231-237 (2005).
9. Kahlem, P., Dorken, B. & Schmitt, C.A. Cellular senescence in cancer treatment: friend or foe? *J. Clin. Invest.* **113**, 169-174 (2004).
10. Schellenberger, E.A.*, et al.* Optical imaging of apoptosis as a biomarker of tumor response to chemotherapy. *Neoplasia* **5**, 187-192 (2003).
11. Dechsupa, S.*, et al.* Quercetin, Siamois 1 and Siamois 2 induce apoptosis in human breast cancer MDA-mB-435 cells xenograft in vivo. *Cancer Biol Ther* **6**, 56-61 (2007).
12. Beekman, C.A.*, et al.* Questioning the value of (99m)Tc-HYNIC-annexin V based response monitoring after docetaxel treatment in a mouse model for hereditary breast cancer. *Applied radiation and isotopes : including data, instrumentation and methods for use in agriculture, industry and medicine* **69**, 656-662 (2011).
13. Lederle, W.*, et al.* Failure of annexin-based apoptosis imaging in the assessment of antiangiogenic therapy effects. *EJNMMI Res* **1**, 26 (2011).
14. Wang, F.*, et al.* Imaging paclitaxel (chemotherapy)-induced tumor apoptosis with 99mTc C2A, a domain of synaptotagmin I: a preliminary study. *Nucl. Med. Biol.* **35**, 359-364 (2008).
15. Zhao, M., Beauregard, D.A., Loizou, L., Davletov, B. & Brindle, K.M. Non-invasive detection of apoptosis using magnetic resonance imaging and a targeted contrast agent. *Nat Med* **7**, 1241-1244 (2001).
16. Smith, B.A.*, et al.* Optical imaging of mammary and prostate tumors in living animals using a synthetic near infrared zinc(II)-dipicolylamine probe for anionic cell surfaces. *J Am Chem Soc* **132**, 67-69 (2010).
17. Smith, B.A.*, et al.* In vivo targeting of cell death using a synthetic fluorescent molecular probe. *Apoptosis* **16**, 722-731 (2011).
18. Xiong, C.*, et al.* Peptide-based imaging agents targeting phosphatidylserine for the detection of apoptosis. *Journal of medicinal chemistry* **54**, 1825-1835 (2011).
19. Ohnishi, S.*, et al.* Intraoperative detection of cell injury and cell death with an 800 nm near-infrared fluorescent annexin V derivative. *Am J Transplant* **6**, 2321-2331 (2006).
20. Al-Ejeh, F.*, et al.* In vivo targeting of dead tumor cells in a murine tumor model using a monoclonal antibody specific for the La autoantigen. *Clin Cancer Res* **13**, 5519s-5527s (2007).
21. Al-Ejeh, F.*, et al.* APOMAB, a La-specific monoclonal antibody, detects the apoptotic tumor response to life-prolonging and DNA-damaging chemotherapy. *PLoS One* **4**, e4558 (2009).
22. Trepel, J., Mollapour, M., Giaccone, G. & Neckers, L. Targeting the dynamic HSP90

complex in cancer. *Nat Rev Cancer* **10**, 537-549 (2010).
23. Wandinger, S.K., Richter, K. & Buchner, J. The Hsp90 chaperone machinery. *J. Biol. Chem.* **283**, 18473-18477 (2008).
24. Lee, C.C., Lin, T.W., Ko, T.P. & Wang, A.H. The hexameric structures of human heat shock protein 90. *PLoS One* **6**, e19961 (2011).
25. Nardai, G., Sass, B., Eber, J., Orosz, G. & Csermely, P. Reactive cysteines of the 90-kDa heat shock protein, Hsp90. *Arch. Biochem. Biophys.* **384**, 59-67 (2000).
26. Park, D., *et al.* Noninvasive imaging of cell death using an Hsp90 ligand. *J Am Chem Soc* **133**, 2832-2835 (2011).
27. Xie, B.W., *et al.* Optical imaging of cell death in traumatic brain injury using a heat shock protein-90 alkylator. *Cell Death Dis* **4**, e473 (2013).
28. Scarlett, J.L., *et al.* Changes in mitochondrial membrane potential during staurosporine-induced apoptosis in Jurkat cells. *FEBS Lett.* **475**, 267-272 (2000).
29. Tafani, M., Minchenko, D.A., Serroni, A. & Farber, J.L. Induction of the mitochondrial permeability transition mediates the killing of HeLa cells by staurosporine. *Cancer Res.* **61**, 2459-2466 (2001).
30. Sauter, B., *et al.* Consequences of cell death: exposure to necrotic tumor cells, but not primary tissue cells or apoptotic cells, induces the maturation of immunostimulatory dendritic cells. *J. Exp. Med.* **191**, 423-434 (2000).
31. Aslakson, C.J. & Miller, F.R. Selective events in the metastatic process defined by analysis of the sequential dissemination of subpopulations of a mouse mammary tumor. *Cancer Res.* **52**, 1399-1405 (1992).
32. Hobbs, S.K., *et al.* Regulation of transport pathways in tumor vessels: role of tumor type and microenvironment. *Proceedings of the National Academy of Sciences of the United States of America* **95**, 4607-4612 (1998).
33. Singh, R.K., *et al.* Organ site-dependent expression of basic fibroblast growth factor in human renal cell carcinoma cells. *The American journal of pathology* **145**, 365-374 (1994).
34. Kashiwagi, S., *et al.* NO mediates mural cell recruitment and vessel morphogenesis in murine melanomas and tissue-engineered blood vessels. *The Journal of clinical investigation* **115**, 1816-1827 (2005).
35. Roberts, W.G., *et al.* Host microvasculature influence on tumor vascular morphology and endothelial gene expression. *The American journal of pathology* **153**, 1239-1248 (1998).
36. Joensuu, H. & Gligorov, J. Adjuvant treatments for triple-negative breast cancers. *Ann. Oncol.* **23 Suppl 6**, vi40-45 (2012).
37. Yang, T.J., Haimovitz-Friedman, A. & Verheij, M. Anticancer therapy and apoptosis imaging. *Experimental oncology* **34**, 269-276 (2012).
38. Taylor, R.C., Cullen, S.P. & Martin, S.J. Apoptosis: controlled demolition at the cellular level. *Nat Rev Mol Cell Biol* **9**, 231-241 (2008).
39. Porter, A.G. & Janicke, R.U. Emerging roles of caspase-3 in apoptosis. *Cell Death Differ.* **6**, 99-104 (1999).
40. Ayukawa, K., *et al.* La autoantigen is cleaved in the COOH terminus and loses the nuclear localization signal during apoptosis. *J. Biol. Chem.* **275**, 34465-34470 (2000).
41. Donoghue, N., Yam, P.T., Jiang, X.M. & Hogg, P.J. Presence of closely spaced protein thiols on the surface of mammalian cells. *Protein Sci* **9**, 2436-2445 (2000).